TRANSITION THRESHOLD AND THE SELF-SUSTAINING PROCESS

Fabian Waleffe[1,2,3] and Jue Wang[1]
[1]*Department of Mathematics, University of Wisconsin, Madison, USA*
[2]*Department of Engineering Physics, University of Wisconsin, Madison, USA*
[3]*CNLS, CCS-2 and IGPP, Los Alamos National Laboratory, USA*
waleffe@math.wisc.edu, wang@math.wisc.edu

Abstract The self-sustaining process is a fundamental and generic three-dimensional nonlinear process in shear flows. It is responsible for the existence of non-trivial traveling wave and time-periodic states. These states come in pairs, an upper branch and a lower branch. The limited data available to date suggest that the upper branch states provide a good first approximation to the statistics of turbulent flows. The upper branches may thus be understood as the "backbone" of the turbulent attractor while the lower branches might form the backbone of the boundary separating the basin of attraction of the laminar state from that of the turbulent state. Evidence is presented that the lower branch states tend to purely streaky flows, in which the streamwise velocity has an essential spanwise modulation, as the Reynolds number R tends to infinity. The streamwise rolls sustaining the streaks and the streamwise undulation sustaining the rolls, both scale like R^{-1} in amplitude, just enough to overcome viscous dissipation. It is argued that this scaling is directly related to the observed R^{-1} transition threshold. These results also indicate that the exact coherent structures never bifurcate from the laminar flow, not even at infinity. The scale of the key elements, streaks, rolls and streamwise undulation, remain of the order of the channel size. However, the higher x-harmonics show a slower decay with R than naively expected. The results indicate the presence of a warped critical layer.

Keywords: wall-bounded turbulence, coherent structures, self-sustaining process, transition threshold, critical layers.

1. INTRODUCTION

Recent pipe flow experiments by Hof et al. (2003) provide clear evidence that the transition threshold, i.e. the smallest perturbation amplitude ϵ that triggers transition from laminar to turbulent flow, scales like R^{-1} as $R \to \infty$, where R is the Reynolds number. Some numerical results also indicate that scaling in plane Couette-like flows and models (e.g. Eckhardt and Mersmann, 1999).

T. Mullin and R.R. Kerswell (eds), Laminar Turbulent Transition and Finite Amplitude Solutions, 85–106.

The concept of transition threshold was introduced by Trefethen et al. (1993) who conjectured that $\epsilon \sim R^a$ with $a < -1$, strictly. Their argument rests on linear transient algebraic growth of some perturbations before exponential viscous decay, i.e. a behavior of the form $\epsilon\, t\, e^{-t/R}$ where ϵ is the initial perturbation amplitude and t is time. Such perturbations grow to a maximum amplitude of order ϵR at a time of order R before the final viscous decay. A simple scaling argument balancing the quadratic nonlinear interaction (since the Navier–Stokes nonlinearity is quadratic) of maximally amplified disturbances with the linear viscous decay of the original disturbance then suggests a transition threshold exponent $a = -3$,

$$(\epsilon R)^2 \sim \frac{\epsilon}{R} \;\Rightarrow\; \epsilon \sim R^{-3}. \tag{1}$$

On the other hand, the balance

$$(\epsilon)^2 \sim \frac{\epsilon}{R} \;\Rightarrow\; \epsilon \sim R^{-1}, \tag{2}$$

suggests that $a = -1$ would correspond to a nonlinear transition where linear transient growth does not play a role. Furthermore, the linear transient growth, which in shear flows primarily results from the redistribution of streamwise velocity by streamwise rolls, is accompanied by a mean shear reduction of order $(\epsilon R)^2$ (Waleffe, 1995a, 1995b, 1997; Reddy et al., 1998). Therefore, for $\epsilon \sim R^{-1}$, that mean shear reduction would invalidate linear theory, since the latter assumes that the mean shear is fixed at its laminar value. Hence, the understated importance of the restriction $a < -1$, *strictly*, in the original conjecture.

A lower bound on the transition threshold was derived by Kreis et al. (1994). That lower bound clearly involves transient growth but leads to the scaling exponent $a = -21/4$, much smaller even than the $a = -3$ suggested by the simple scaling argument above (1). Numerical simulations suggest scaling exponents that are much closer to $a = -1$. Reddy et al. (1998) report $a \approx -1$ for streamwise vortices perturbations and $a \approx -5/4$ for oblique roll perturbations, in plane Couette flow, and $a \approx -7/4$ for both type of perturbations in plane Poiseuille flow. However, those exponents are deduced from small and low Reynolds number ranges and may therefore not correspond to the true asymptotic values. Chapman (2002) presents an asymptotic scaling analysis of the two transition scenarios studied in Reddy et al. (1998)) and suggests that the true scaling exponents are in fact $a = -1$ for both types of perturbations in plane Couette flow, and $a = -3/2$ and $-5/4$ for the streamwise vortices and oblique perturbations, respectively, in plane Poiseuille flow.

Chapman's study contains a detailed asympotic analysis of the linear dynamics about the laminar flow using WKB methods.[1] However, the rest of his formal analysis consists only of scaling estimates and is incomplete. His

analysis of oblique perturbations calls on intricate initial disturbances with relatively large vorticity of $O(R^{-2/3})$ in plane Couette flow and $O(R^{-11/12})$ in plane Poiseuille flow and specific nonlinear interactions to create channel-size streamwise rolls.[2] His analysis of the streamwise vortex scenario leads to plausible thresholds for streak instability, but those cannot be considered as thresholds for transition since his formal analysis does not address feedback.[3] Transition is not possible without feedback. The instability of a transient perturbation, e.g. the instability of transient streaks, is not sufficient for transition, since that instability would necessarily extract energy from the streaks and therefore could simply accelerate the return to the laminar flow. Transition claims require demonstrating that disturbances are sustained.

The *self-sustaining process* (SSP) is a weakly nonlinear theory about a spanwise varying shear flow that incorporates feedback. It is a synthesis of experimental studies of coherent structures in the near-wall region of turbulent flows (particularly the nicely illustrated work of Acarlar and Smith (1987)) and theoretical ideas due to Benney (1984). The main elements of the SSP (Figure 1) are streamwise rolls of $O(R^{-1})$ that redistribute the streamwise velocity to create $O(1)$ streaks whose streamwise undulation of $O(R^{-1})$ directly feeds back onto the streamwise rolls (Waleffe, 1990, 1995a, b, 1997; Waleffe et al., 1993). The validity and relevance of the SSP was established by Hamilton et al. (1995) using Direct Numerical Simulations which strongly suggested the existence of time-periodic solutions in plane Couette flow that have been isolated by Kawahara and Kida (2001). The process and the proposed scalings have served as the basis for a method to compute three-dimensional traveling wave solutions of the Navier–Stokes equations. In that method (Waleffe, 1998), an artificial forcing of $O(R^{-2})$ is introduced to sustain $O(R^{-1})$ streamwise rolls, these rolls redistribute the mean shear to create $O(1)$ streaks. The resulting new steady state, called the streaky flow, is linearly unstable because of the strong spanwise inflections. This instability is subcritical in terms of the artificial forcing because the direct nonlinear effect of the streak instability is to feedback on the streamwise rolls. The nonlinear self-interaction of an $O(R^{-1})$ streak eigenmode provides an $O(R^{-2})$ nonlinear forcing that replaces the artificial forcing to sustain the rolls against viscous decay. That approach was used successfully in plane Couette and Poiseuille flow with both free-slip and no-slip boundary conditions (Waleffe, 1998, 2001, 2003) and has also been used to compute analogous traveling waves in pipe flow by Faisst and Eckhardt (2003) and Wedin and Kerswell (2004). Itano and Toh (2001) use a related shooting method where the starting point is a suitably selected x-averaged flow (i.e. a streaky flow) obtained from a direct numerical simulation. These works demonstrate that the SSP is robust and generic for shear flows.

The more recent and farther-reaching work on transient growth (e.g. Reddy et al., 1998; Chapman, 2002) has moved closer to the self-sustaining process

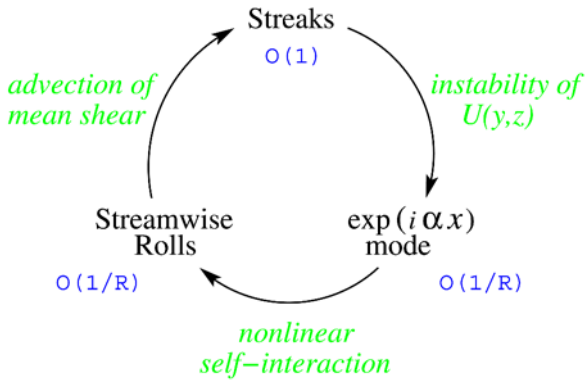

Figure 1. The key elements of the Self-Sustaining Process with their presumed scalings.

theory. Those papers do not focus anymore on which laminar flow perturbations lead to maximum transient energy growth but instead on those perturbations that lead to the most unstable streaks.[4] However that line of work has not yet addressed the feedback issue which is key for transition. Work on the self-sustaining process includes the complete and exact representation of the redistribution of streamwise velocity by streamwise rolls, including the modification of the mean shear, and seeks to construct streamwise rolls leading to streaks whose spanwise inflectional instability leads *directly* to the regeneration of the *same* streamwise rolls, thereby demonstrating self-sustenance and transition potential.

Here, motivated by Hof, Juel and Mullin's recent outstanding evidence that $a = -1$ in pipe flow, we look back at the presumed scalings for the self-sustaining process and provide numerical evidence that such scalings are asymptotically exact as $R \to \infty$. We illustrate the ideas using a simple 4th order model, follow with a sketch of an asymptotic theory and finally present fully resolved calculations of the lower branch exact coherent states in plane Couette flow. Our Cartesian coordinates follow the usual choice with x streamwise, y shearwise (wall-normal) and z spanwise, and corresponding velocity components u, v and w, respectively.

2. SCALING IN A SIMPLE MODEL OF THE SSP

A simple model of the self-sustaining process was proposed in Waleffe (1995a, 1995b) and later "derived" from a systematic Galerkin projection of the Navier–Stokes equations (Waleffe, 1997). The simplest non-trivial Galerkin model consists of 8 modes, but that model is pathological as explained in Waleffe (1997, sect. IV). An *ad hoc* reduction to a 4-mode model was made in Waleffe (1997). Moehlis et al. (2004) have considered a 9-mode model

that cures the pathological behavior of the 8-mode model, to some extent. Their surgical modification of the 8-mode model is along the lines suggested in Waleffe (1997, sect. IV), namely, to increase the resolution in the wall-normal direction, but they do this in a very economical way that only adds one mode and slightly modifies the shearwise structure of a few other modes. Their 9-mode models illustrates some of the nonlinear dynamics of shear flow transition such as chaotic repellors and the fractal nature of the transition boundary. However, from the point of view of the gross features of self-sustaining process and the associated non-trivial fixed points, the original 4th order model is sufficient and simpler.

The 4th order model[5] consists of the 4 real ODEs

$$\begin{array}{lcccccc}
\left(\dfrac{d}{dt}+\dfrac{\kappa_m^2}{R}\right)M &=& \frac{\kappa_m^2}{R} & -\sigma_u\,UV & & +\sigma_m\,W^2 \\
\left(\dfrac{d}{dt}+\dfrac{\kappa_u^2}{R}\right)U &=& & \sigma_u\,MV & -\sigma_w\,W^2 & \\
\left(\dfrac{d}{dt}+\dfrac{\kappa_v^2}{R}\right)V &=& & & \sigma_v\,W^2 & \\
\left(\dfrac{d}{dt}+\dfrac{\kappa_w^2}{R}\right)W &=& & \sigma_w\,UW & -\sigma_v\,VW & -\sigma_m\,MW
\end{array} \tag{3}$$

In this model, the κ^2/R terms on the left-hand side represent viscous dissipation, all σ coefficients on the right-hand side are considered to be positive. We do not need to consider specific numerical values for the κ's and σ's. The right-hand side terms are organized in columns to emphasize that the nonlinear terms are energy-conserving and to clearly identify the various parts of the SSP. The first column κ_m^2/R is the external forcing of the mean shear amplitude $M(t)$. The 2nd column correspond to the redistribution of the mean shear by streamwise rolls of amplitude $V(t)$ to create streaks of amplitude $U(t)$. The flip-side of that redistribution is the Reynolds stress $-\sigma_u UV$ in the M-equation. The third column represents the streak instability. $W(t)$ is the amplitude of a three-dimensional streak eigenmode, sinusoidal in the streamwise x-direction, that would grow exponentially on sufficiently large amplitude (frozen) streaks U. This is accompanied by a Reynolds stress arising from the nonlinear self-interaction of the streak eigenmode, $-\sigma_w W^2$, that destroys the streaks as discussed in the introduction. The 4th column is the key nonlinear feedback on the streamwise rolls, $\sigma_v W^2$, that arises from the nonlinear self-interaction of the streak eigenmode. The fifth column was overlooked in the original write-up of the SSP model (Waleffe, 1995a, 1995b), since it is not essential for the SSP. Its existence was revealed by the Galerkin derivation and it turns out to be essential for the lower branch scaling discussed in this article, as already discussed in Waleffe (1997, eqn. (23)). Its physical origin is simply the

shearing by the mean of x-dependent disturbances. This shearing is important and tied to the reduction of the mean shear by the streaks-rolls Reynolds stress. Indeed if $\sigma_w U - \sigma_m M < 0$, i.e. if the streaks are not sufficiently large compared to the mean shear, then the streak instability (the exponential growth of W) cannot occur. Note that the rolls V also reduce the streak instability growth rate, but they are typically much weaker than the streaks U and the mean shear M.

Model (3) has a laminar fixed point $(M, U, V, W) = (1, 0, 0, 0)$ that is linearly stable for all R, as in plane Couette flow. It can be shown in general, i.e. for any κ's and σ's provided that all σ's are positive, that model (3) has a critical Reynolds number $R_{sn} > 0$ above which two non-trivial fixed points exist as long as $\sigma_u\sigma_v\sigma_w > 0$. The complete derivation is sketched in Waleffe (1997, sect. III D); here we only state the asymptotic balance for the lower branch fixed point. For large R, the lower branch fixed point (indicated by the subscript ℓ) corresponds to the balance

$$\begin{array}{lcl} \dfrac{\kappa_m^2}{R} M_\ell & \sim & \frac{\kappa_m^2}{R} \quad -\sigma_u\, U_\ell\, V_\ell \\ \dfrac{\kappa_u^2}{R} U_\ell & \sim & \sigma_u\, M_\ell\, V_\ell \\ \dfrac{\kappa_v^2}{R} V_\ell & \sim & \sigma_v\, W_\ell^2 \\ \sigma_w\, U_\ell & \sim & \sigma_m\, M_\ell \end{array} \tag{4}$$

specifically,

$$\lim_{R\to\infty} M_\ell = \frac{1}{1 + \dfrac{\kappa_u^2 {\sigma_m}^2}{\kappa_m^2 \sigma_w^2}} < 1, \qquad \lim_{R\to\infty} U_\ell = \frac{\sigma_m/\sigma_w}{1 + \dfrac{\kappa_u^2 {\sigma_m}^2}{\kappa_m^2 \sigma_w^2}} > 0, \tag{5}$$

$$\lim_{R\to\infty} (R\, V_\ell) = \frac{\sigma_m \kappa_u^2}{\sigma_u \sigma_w}, \qquad \lim_{R\to\infty} (R\, W_\ell) = \sqrt{\frac{\sigma_m \kappa_u^2 \kappa_v^2}{\sigma_u \sigma_v \sigma_w}} \tag{6}$$

so the lower branch fixed point tends to a streaky flow, not to the laminar point as $R \to \infty$, $(M_\ell, U_\ell, V_\ell, W_\ell) \to (M_\infty, U_\infty, 0, 0) \neq (1, 0, 0, 0)$. This is only true if $\sigma_m \neq 0$. Thus the key physical effect responsible for the R^{-1} scaling of streamwise rolls and streak eigenmode, and the need for $O(1)$ streaks, is the shearing of the x-dependent streak eigenmode by the mean shear.[6]

2.1 Transition threshold in the 4th order model

The transition threshold is the smallest distance to the stable manifold of the lower branch coherent state.[7] Therefore we want to estimate the smallest initial condition that will bring the system in the neighborhood of the lower branch

fixed point. Our postulate is that we can obtain a good estimate of that threshold from the lower branch coherent state combined with our mechanistic understanding of the self-sustaining process.

A look at the 4th order model (3) shows that $W = 0$ is an invariant manifold. This follows from the fact that W represents the amplitude of the only x-dependent 3D mode in that model. The streaks U and rolls V correspond to x-independent 2D modes and the mean shear M is a 1D mode with no streamwise or spanwise variation. Therefore this $W = 0$ invariant manifold directly correspond to the 2D x-independent invariant manifold for the Navier–Stokes equations. It is clear that the laminar fixed point is the global attractor in the $W = 0$ invariant manifold, since V is not sustained and will decay viscously back to zero, in which case the streamwise velocity redistribution ceases and $U \to 0$, $M \to 1$. This is true also for the 2D invariant manifold in shear flows, as first shown in Joseph and Tao (1963). Therefore, to trigger transition in model (3), the initial conditions must be such that $W(0) \neq 0$. This is a first key observation and constraint for transition.

Besides the need for $W(0) \neq 0$, it is rather clear that an efficient way to jumpstart the SSP is to start with streamwise rolls $V(0) \sim V_\ell = O(R^{-1})$ with $V(0) \gg W(0) \neq 0$ and $V(0) > V_\ell$ since the rolls will suffer some viscous decay while creating streaks. This is the strategy that has always been employed to study the SSP (e.g. Waleffe, 1995a, sect. 4.1; Waleffe, 1997, sect. II A) as well as to calculate self-sustained 3D traveling waves in the Navier–Stokes equations by bifurcation from a streaky flow. Another good candidate perturbation is to start with a $W(0) \sim W_\ell = O(R^{-1})$. However such initial condition is subjected to shearing by the mean ($-\sigma_m MW$ term) which destroys W rapidly. Therefore we expect this type of perturbation to be much less effective in triggering transition, requiring $W(0)$ significantly larger than W_ℓ although still scaling like R^{-1} asymptotically as $R \to \infty$.

3. ASYMPTOTIC THEORY OF THE SSP

The original presumed scalings for the SSP was that streamwise rolls of $O(R^{-1})$ create inflectionally unstable streaks of $O(1)$, and that the nonlinear self-interaction of $O(R^{-1})$ streak eigenmode, sinusoidal in x, sustains the rolls.

To formalize these scaling presumptions we begin with the postulate that lower branch traveling wave states correspond to the following naive asymptotic scaling for each of the Cartesian velocity components and the pressure:

$$\begin{aligned} u &= u_0 + R^{-1}u_1 e^{i\theta} + R^{-2}u_2 e^{2i\theta} + c.c. + \cdots \\ v &= R^{-1}v_0 + R^{-1}v_1 e^{i\theta} + R^{-2}v_2 e^{2i\theta} + c.c. + \cdots \\ w &= R^{-1}w_0 + R^{-1}w_1 e^{i\theta} + R^{-2}w_2 e^{2i\theta} + c.c. + \cdots \\ p &= R^{-2}p_0 + R^{-1}p_1 e^{i\theta} + R^{-2}p_2 e^{2i\theta} + c.c. + \cdots \end{aligned} \tag{7}$$

where $\theta = \alpha(x - ct)$, $c = c(\alpha, R)$ is a real phase velocity and $c.c.$ stands for complex conjugate. Every modal amplitude function, e.g. $u_0 = u_0(y, z; \alpha, R)$ is a 2D function of both y and z. The streamwise wavenumber α and the Reynolds number R are the controlling parameters.

This asymptotic *ansatz* is very similar to that postulated by Benney (1984). Benney's original formulation was for time-dependent inviscid flow with an amplitude parameter ϵ in lieu of R^{-1} and long time and space modulations, $T = \epsilon t$, $X = \epsilon x$. Benney and Chow (1989) later re-introduced the Reynolds number, which requires the semi-implicit assumption that $\epsilon = O(R^{-1})$.

Substituting expansion (7) into the Navier–Stokes equations leads to the following coupled equations at lowest order:

Streaky flow

$$\nabla^2 u_0 = v_0 \frac{\partial u_0}{\partial y} + w_0 \frac{\partial u_0}{\partial z} \quad + \; F_0, \tag{8}$$

First x-harmonic

$$\begin{aligned} (u_0 - c)\frac{\partial \boldsymbol{v}_1}{\partial x} + (\boldsymbol{v}_1 \cdot \boldsymbol{\nabla} u_0)\hat{\boldsymbol{x}} &= -\boldsymbol{\nabla}\left(p_1 e^{i\theta}\right), \\ \boldsymbol{\nabla} \cdot \boldsymbol{v}_1 &= 0, \end{aligned} \tag{9}$$

Streamwise rolls

$$\begin{aligned} \nabla^4 \Psi_0 = J(\nabla^2 \Psi_0, \Psi_0) \quad + \\ 2\frac{\partial^2}{\partial y \partial z}\left(v_1 v_1^* - w_1 w_1^*\right) + \left(\frac{\partial^2}{\partial z^2} - \frac{\partial^2}{\partial y^2}\right)\left(v_1 w_1^* + v_1^* w_1\right), \end{aligned} \tag{10}$$

where $\Psi_0(y, z)$ is the streamfunction for the streamwise rolls $(0, v_0, w_0)$ with

$$v_0(y, z) = \frac{\partial \Psi_0}{\partial z}, \quad w_0(y, z) = -\frac{\partial \Psi_0}{\partial y}, \tag{11}$$

$J(A, B) = \partial A/\partial y \;\; \partial B/\partial z - \partial A/\partial z \;\; \partial B/\partial y$ is the usual Jacobian and $\boldsymbol{v}_1 = e^{i\theta}(u_1 \hat{\boldsymbol{x}} + v_1 \hat{\boldsymbol{y}} + w_1 \hat{\boldsymbol{z}})$ is the first harmonic with $\hat{\boldsymbol{x}}$, $\hat{\boldsymbol{y}}$ and $\hat{\boldsymbol{z}}$ the unit vectors in the respective coordinate directions. The streaky flow equation (8) contains the non-dimensionalized driving pressure gradient F_0. For channel (plane Poiseuille) flow, $F_0 = -2$ with $-1 \le y \le 1$ and $u_0(\pm 1, z) = 0$, while $F_0 = 0$ with $u_0(\pm 1, z) = \pm 1$ for plane Couette. Equations (8), (9), (10) are the equations for the lowest order terms in a Reynolds number expansion of the modal amplitudes, e.g. for the u_{00} term in the expansion

$$u_0(y, z; \alpha, R) = u_{00}(y, z; \alpha) + \frac{1}{R} u_{01}(y, z; \alpha) + \cdots \tag{12}$$

but we write u_0 for brevity. The lowest order problem consists of three coupled two-dimensional (y and z) problems (8), (9), (10).

The lowest order contribution to the 2nd harmonic would arise at order R^{-2}

$$\begin{aligned}(u_0 - c)\frac{\partial \boldsymbol{v}_2}{\partial x} + (\boldsymbol{v}_2 \cdot \nabla u_0)\hat{\boldsymbol{x}} &= -\nabla\left(p_2 e^{i2\theta}\right) - \nabla \cdot (\boldsymbol{v}_1 \boldsymbol{v}_1) \\ \nabla \cdot \boldsymbol{v}_2 &= 0\end{aligned} \tag{13}$$

where $\boldsymbol{v}_2 = e^{i2\theta}(u_2\hat{\boldsymbol{x}} + v_2\hat{\boldsymbol{y}} + w_2\hat{\boldsymbol{z}})$ is the 2nd harmonic.

Equations (8), (9), (10) are the Navier–Stokes equivalent of the asymptotic balance (4) for the lower branch of the 4th order model. Equation (8) corresponds to the first two equations of that model, and to the advective redistribution of the streamwise velocity by streamwise rolls to induce an essential spanwise modulation. Equation (10) directly corresponds to the 3rd equation in (4), with the streamwise rolls maintained by the quadratic self-interaction of the streak eigenmode. Equations (9) correspond to the linearized equations – if $u_0(y, z)$ was fixed – for the stability of the 2D streaky flow $u_0(y, z)$ to a 3D perturbation, $\boldsymbol{v}_1$, sinusoidal in x. Since we demand that c be real, these equations correspond to the *marginal* inviscid stability of a pure streaky flow, just as the 4th equation of (4). Note that equations (8) and (10) are viscously balanced (formally corresponding to $R = 1$ in fact), while Equation (9) is inviscid, with $\boldsymbol{v}_1$ corresponding to a marginally stable mode, and requires only inviscid boundary conditions. In a wall-bounded domain, this suggests that viscous boundary layers of $O(R^{-1/2})$ will be required to satisfy the no-slip boundary conditions. There is also the possibility that a *critical layer* will arise from the

$$u_0(y, z) - c = 0 \tag{14}$$

singularity in the 1st harmonic equation (9). In two dimensions, linear critical layers scale like $R^{-1/3}$ while nonlinear critical layers scale like $\epsilon^{1/2}$ where ϵ is a measure of the disturbance amplitude (e.g. Maslowe, 1986). These scalings are for small 2D perturbation of the 1D laminar shear flow. In our case, our critical layer $u_0(y, z) - c = 0$ would be a warped surface, our perturbation is 3D and its amplitude is directly tied to the Reynolds number as $\epsilon = R^{-1}$. Nonetheless, by analogy with 2D critical layers we can expect a warped critical layer of thickness δ with

$$\epsilon^{1/2} = R^{-1/2} \lesssim \delta \lesssim R^{-1/3}. \tag{15}$$

Such critical and boundary layers seriously complicate the expansion, both theoretically and computationally. Looking at the right-hand side of the 2nd harmonic equation (13), the nonlinear forcing term arising from the the 1st harmonic, $\nabla \cdot (\boldsymbol{v}_1 \boldsymbol{v}_1)$, could contribute at order $R^{-5/3}$ or $R^{-3/2}$ instead of R^{-2} as postulated. This is because if the first harmonic has amplitude of order R^{-1}, then its nonlinear self-interaction term, $\boldsymbol{v}_1 \boldsymbol{v}_1$, would indeed be of order R^{-2}, but if a critical layer of thickness δ is present, then the nonlinear forcing term $\nabla \cdot (\boldsymbol{v}_1 \boldsymbol{v}_1)$ could generate a 2nd harmonic of order $\delta^{-1}R^{-2}$. For δ as in (15) this gives 2nd harmonic amplitudes between $R^{-5/3}$ and $R^{-3/2}$.

4. NUMERICAL CONTINUATION OF LOWER BRANCH STATES

Here we present fully-resolved numerical solutions of the Navier–Stokes equations that consist of lower branch 'exact coherent structures' in plane Couette flow with no-slip boundary conditions. These particular solutions have $c = 0$ by symmetry in a Galilean frame such that the average flow velocity is zero. These solutions were obtained in two ways, (1) by homotopy from free-slip to no-slip solutions (Waleffe, 2003), the free-slip solutions having been obtained using the bifurcation from streaky flow approach (Waleffe, 1998), and (2) by direct bifurcation from a streaky flow in the no-slip case. These no-slip solutions belong to the same family as the solutions originally obtained by Nagata (1990) by continuation of wavy Taylor vortices solutions in rotating plane Couette flow.

4.1 Bifurcation from streaky flow in no-slip plane Couette

For the SSP approach of tracking solutions that bifurcate from a streaky flow, we begin by adding an artificial forcing of the streamwise rolls to the Navier–Stokes equations. The forcing is chosen to correspond to the slowest decaying linear streamwise rolls appropriate to the shear layer. In the no-slip plane Couette case, these correspond to x-independent vertical velocity of the form

$$V(y,z) = \frac{F_r}{R}\frac{\hat{v}(y)}{\hat{v}_m}\cos\gamma z = \frac{1}{R}\frac{\partial\Psi_0}{\partial z} \tag{16}$$

with

$$\hat{v}(y) = \frac{\cos\beta y}{\cos\beta} - \frac{\cosh\gamma y}{\cosh\gamma} \tag{17}$$

where $\hat{v}_m = \max_y\left[\hat{v}(y)\right]$ and β is the smallest positive solution of $\beta\tan\beta + \gamma\tanh\gamma = 0$. For $\gamma = 5/3$, $\beta \approx 2.604189715$. The functions (17) solve the Stokes eigenvalue problem $(D^2-\gamma^2)^2\hat{v} = \lambda(D^2-\gamma^2)\hat{v}$, with $\hat{v} = D\hat{v} = 0$ at $y = \pm 1$, where $D = d/dy$. The streamwise rolls are normalized so that $\max V(y,z) = F_r/R$ where R is the Reynolds number and F_r is an $O(1)$ forcing parameter. These are the same streamwise rolls as used in Waleffe (1997). The free-slip rolls used in Waleffe (1998) have the same form and scaling except that $\hat{v}(y) = \cos\pi y/2$ in that case.

In that formulation, the initial roll forcing must balance the viscous term in the streamwise rolls equation (10). For $v = V(y,z)$ as in (16)

$$\nabla^4\Psi_0(y,z) = F_r\,\frac{(\beta^2+\gamma^2)^2}{\hat{v}_m}\frac{\cos\beta y}{\cos\beta}\,\frac{\sin\gamma z}{\gamma}, \tag{18}$$

and we therefore add the right-hand side of this equation as a forcing term to the RHS of the streamwise rolls equation (10) (the R^{-2} scaling of the forcing term

is implicit in that equation). In the free-slip case, the Jacobian $J(\nabla^2\Psi_0, \Psi_0)$, corresponding to the nonlinear self-advection of the zeroth harmonic in (10) vanishes identically. That nonlinear term does not vanish in the no-slip case with the forcing (18), however it is small and has little effect. In the no-slip case, that forcing generate rolls that are only approximately described by (16). This is of no consequence, since the forcing is merely an educated guess for the streamwise rolls.

The roll forcing sustains weak streamwise rolls that redistribute the streamwise velocity and the base state now consists of a two-dimensional, three-component "streaky flow" $[u_0(y, z), R^{-1}v_0(y, z), R^{-1}w_0(y, z)]$ instead of the one-dimensional, one-component laminar flow $[U(y), 0, 0]$. That streaky flow is linearly unstable and we can track the bifurcating solution from the marginal stability point. The bifurcation is subcritical in term of the roll-forcing parameter, confirming that the first-harmonic nonlinear self-interaction terms on the RHS of (10) positively feedback on the rolls and take over the role of the artificial roll forcing. For that continuation of 3D solutions from the bifurcation point of the streaky flow, F_r is a dependent variable that must be computed and we select

$$A_x = \Re\langle \eta e^{-i\alpha x}\rangle \tag{19}$$

as the new control parameter where $\langle\cdot\rangle$ denotes an average over the domain and $\Re$ denotes real part. Hence, A_x is the y-average of the $(\alpha, 0)$ Fourier component of the y-vorticity η. That control parameter is chosen because it is a key component of the sinusoidal streak instability mode. Figure 2 shows the resulting bifurcation diagrams for several (α, γ) and R. The key objective is to obtain a 3D self-sustained solution at $F_r = 0$. Once a solution has been obtained, it can be continued in the self-sustained parameter space (α, γ, R) with $F_r = 0$. Details of the mathematical and numerical formulation can be found in Waleffe (2003) and the resolution parameters quoted below correspond to the numerical parameters $[L_T, M_T, N_T]$ in that reference.

4.2 Continuation of lower branch solutions to high R

We pick the fundamental wavenumbers $\alpha = 1.14$ and $\gamma = 2.505$, corresponding to spatial periods $L_x = 2\pi/\alpha$ and $L_z = 2\pi/\gamma$. These parameter values follow from our earlier studies of the SSP and exact coherent states in plane Couette flow. The value $\gamma = 5/3 \approx 1.67$ was selected and $\alpha \approx 1.14$ obtained by "annealing" studies of plane Couette turbulence in Hamilton et al. (1995) that confirmed the validity of the SSP and suggested the existence of a time-periodic solution for those parameter values at $R = 400$ extracted in Kawahara and Kida (2001). A continuation study of 3D steady states in Waleffe (2002) found that these states exist only for $\alpha \lesssim 1.08$ when $\gamma = 1.67$ and for $1.7 \lesssim \gamma$ when $\alpha = 1.14$, at small Reynolds numbers $\lesssim 400$. In

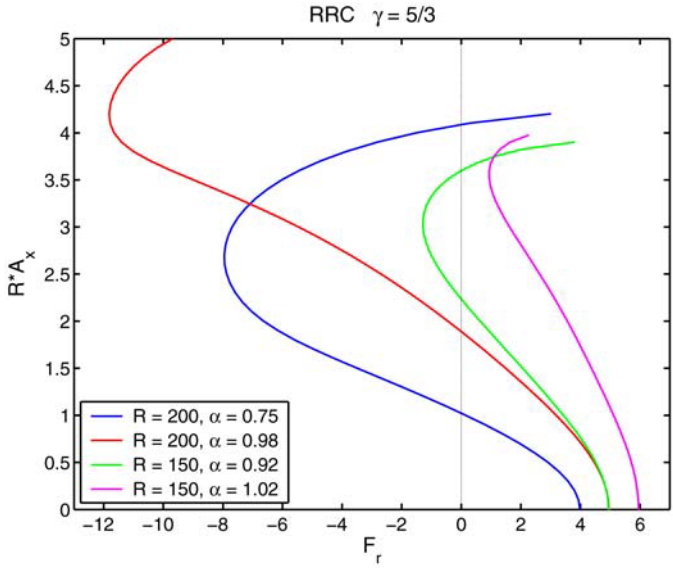

Figure 2. Bifurcation diagrams for no-slip streaky plane Couette flow with $\gamma = 1.67$ (resolution [9,21,9]). Vertical axis is A_x defined in (19) multiplied by R.

particular, 3D steady states were found to exist at $R = 400$ when $\alpha = 1.14$ for $\gamma = 1.5 \times 1.67 = 2.505$ and $\gamma = 2 \times 1.67 = 3.34$. The latter corresponds to the 2nd z-harmonic in a box of fundamental spanwise wavenumber $\gamma = 1.67$, while the former is intermediate between the fundamental and the 2nd harmonic. We selected $\alpha = 1.14$ and $\gamma = 2.505$ for our initial lower branch continuation to large Reynolds numbers but have also considered other parameter values such as $(\alpha, \gamma) = (1.14, 2.5)$, $(1.39, 2.5)$ and $(1, 2)$, all with similar results.

Figure 3 visualizes the typical structure of the lower branch steady state at high R. The streaks (visualized by the green isosurface of total streamwise velocity u) appear completely straight, i.e. x-independent. The red isosurfaces correspond to $Q = 0.6 \max(Q) = 3.46\,10^{-4}$ where $Q = \nabla^2 p/2$ is the 2nd invariant of the velocity gradient tensor. Note that although the red Q-isosurfaces are prominent in the figure, they correspond to very low values of max Q, consistent with the presumption that rolls and streak undulation are of $O(R^{-1})$. The yellow isosurface is $u = 0$ and this correspond to the critical surface $u_0(y, z) - c = 0$, since $c = 0$ by symmetry for these plane Couette flow steady states and $u \approx u_0(y, z)$. It is remarkable how the Q isosurface straddles that $u = 0$ surface, suggesting that it is indeed a critical layer.

Figure 4 shows the mean velocity profile (i.e. the x and z average streamwise velocity) for the lower branch steady states for $(\alpha, \gamma) = (1.14, 2.505)$ at $R =$

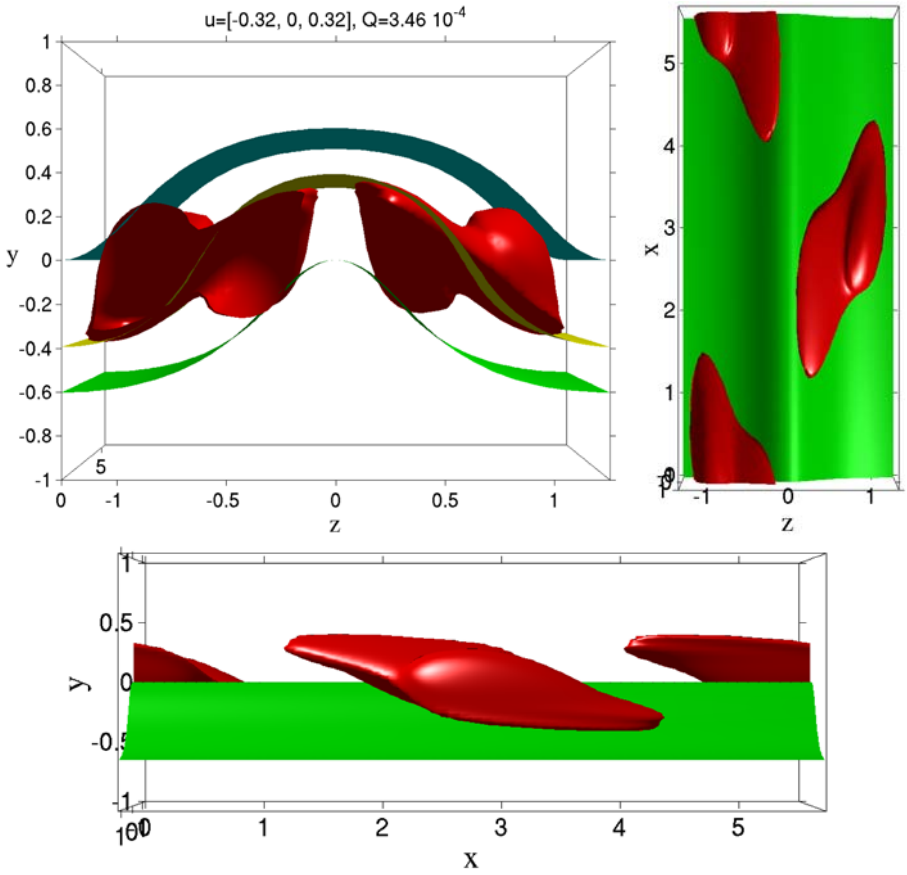

Figure 3. Isosurfaces $u = -0.32$ (green), 0 (yellow), 0.32 (cyan) and $Q = \nabla^2 p/2 = 0.6\max(Q) = 3.46 \times 10^{-4}$ (red) for $(\alpha, \gamma, R) = (1.14, 2.505, 6196)$, resolution [9, 75, 21]. Clockwise: Front, top and side views. Top and side show Q and $u = -0.32$ only.

400, 897 and 7050. Although the higher R profiles are closer to laminar they do not seem to tend to the laminar flow as $R \to \infty$, in fact the profiles are very weakly dependent on R, which is why we jump from $R = 897$ to 7050 in the figures. The mean profiles for $(\alpha, \gamma) = (1, 2)$ at $R = 400$, 867 and 7014 are also shown.

Figure 5 shows the x-averaged, z-rms velocity fluctuation profiles, i.e. the rms of the streaks, defined as the x-averaged streamwise velocity minus the mean velocity, and of the streamwise rolls. The latter are scaled by a factor of R. Those profiles show that the streaks appear to be converging to an $O(1)$ profile, while the rolls scale like R^{-1}. The z-rms velocity profiles for the 1st harmonic, scaled by R, are shown in Figure 6. These R-compensated profiles appear to show convergence, confirming the R^{-1} scaling of the first harmonic.

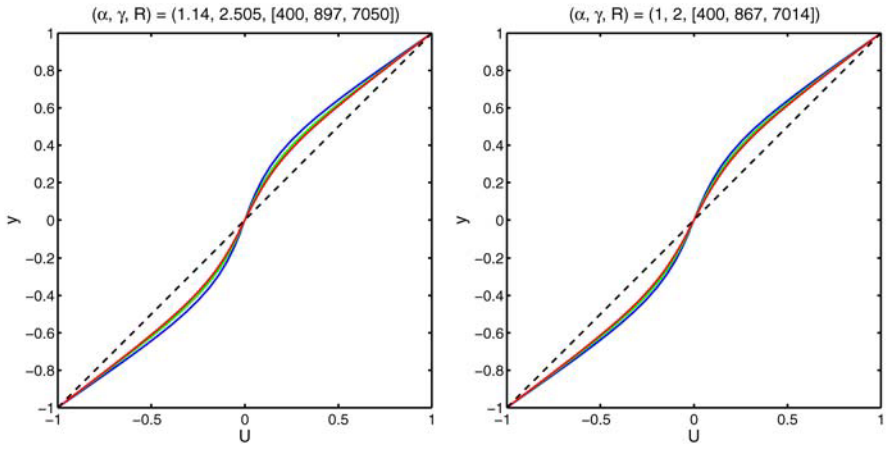

Figure 4. Mean velocity profiles for lower branch steady states in no-slip plane Couette. Left: $(\alpha, \gamma) = (1.14, 2.505)$ for $R = 400, 897, 7050$ (higher R closer but not converging to laminar), resolution [13, 27, 13], [9, 45, 17] and [9, 75, 21], respectively. Right: $(\alpha, \gamma) = (1, 2)$ for $R = 400, 867, 7014$.

Although, there are signs of boundary layers near the walls in the u_1 and w_1 profiles, the most dramatic feature is the rapid rise of the profiles away from the walls near $y = \pm 0.4$. This roughly corresponds to the extreme y-locations of the critical surface $u_0(y, z) - c = 0$ show in Figure 3. That critical surface is very weakly dependent on the Reynolds number R as confirmed by the mean and rms-streak profiles in Figures 4 and 5. This critical layer interpretation is confirmed by the rms profiles of the 2nd harmonic shown in Figure 7. Those profiles are scaled by $R^{3/2}$ and appear to be converging. The most dramatic feature is that they are close to zero near the walls but then shoot up abruptly near $y = \pm 0.4$ again. This behavior, together with the apparent $R^{-3/2}$ scaling instead of the naive R^{-2}, strongly suggest that critical layer behavior is taking place. Log-log plot of the peak rms values for the streamwise rolls, the 1st, 2nd and 3rd harmonics are shown in Figure 8 together with a lin-lin plot of the peak rms streak amplitude. These plots provide a global visual confirmation that the rolls and the first harmonic scale like R^{-1}. The 2nd harmonic appears to scale like $R^{-3/2}$ and the 3rd like R^{-2}. This is in contrast to the R^{-2} and R^{-3}, respectively, in the naive expansion (7) and an indication that critical and/or boundary layers are occuring. The earlier figures suggest the key importance of the critical surface $u_0(y, z) - c = 0$. We have verified that $R^{-3/2}$ and R^{-2} are better fits than $R^{-5/3}$ and $R^{-7/3}$ for the 2nd and 3rd harmonic, respectively. The bottom plots in Figure 8 show the peak rms streak amplitude for $(\alpha, \gamma) = (1.14, 2.505)$, $(1.39, 2.5)$, $(1, 2)$ and strongly suggest convergence

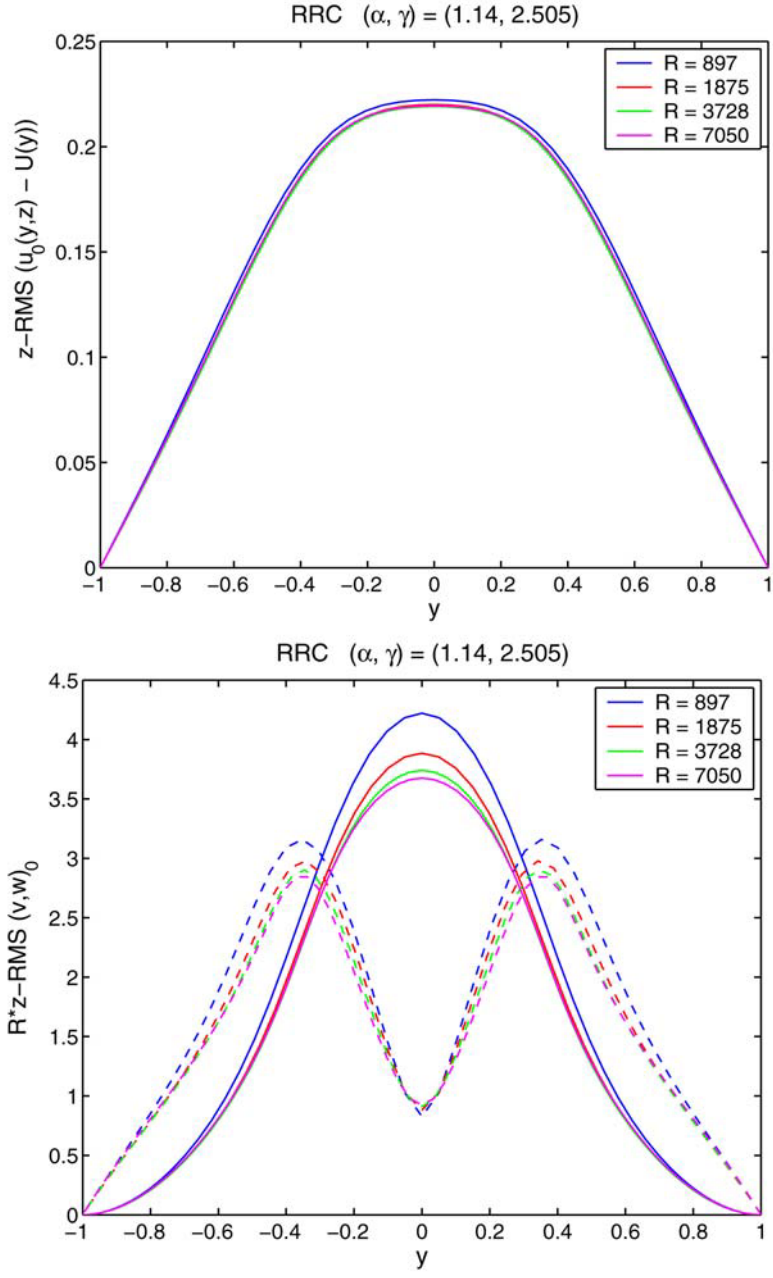

Figure 5. z-RMS of x-averaged velocity fluctuation profiles. Top: streaks $u_0(y, z) - \bar{u}(y)$. Bottom: rolls scaled by R, v_0 solid, w_0 dash. Peak rms values decrease with increasing R.

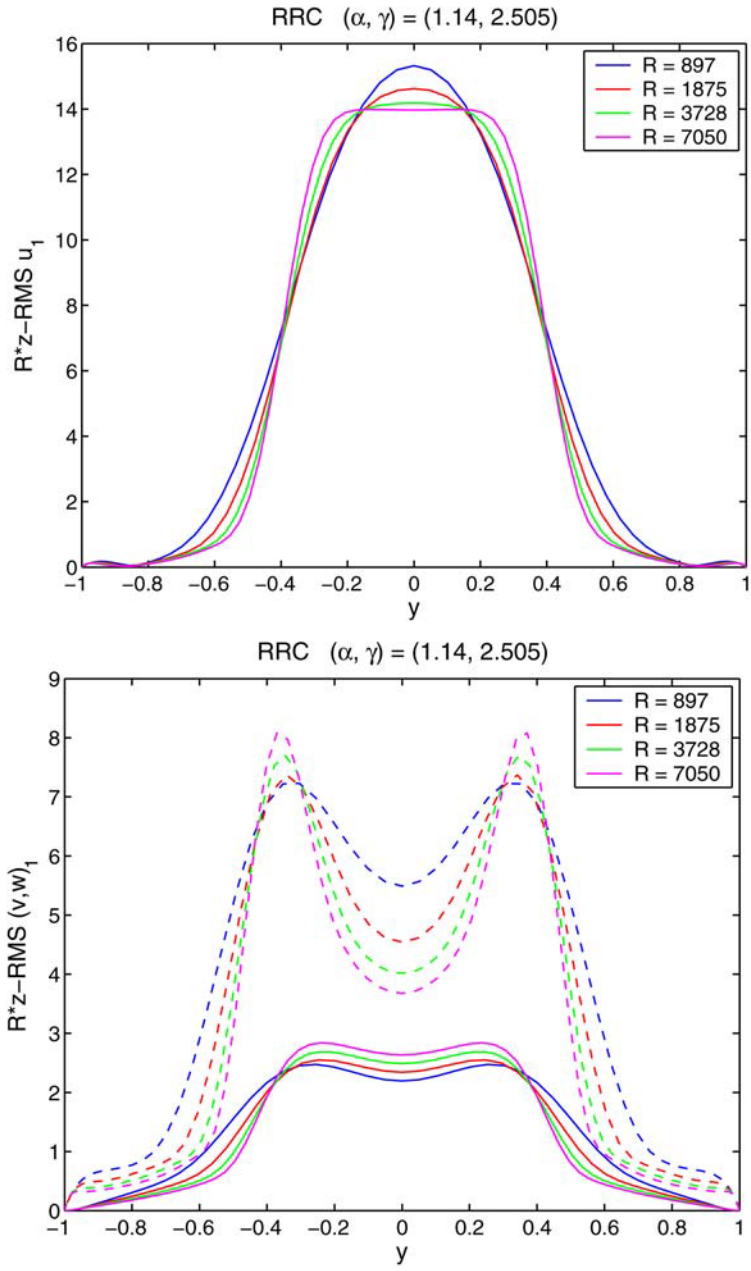

Figure 6. z-RMS velocity profiles scaled by R for the 1st harmonic $\boldsymbol{v}_1$. Top: streamwise velocity $u_1(y, z)$. Bottom: v_1 solid, w_1 dash. Peak scaled rms decreases for u_1 but increases for v_1, w_1 as R increases.

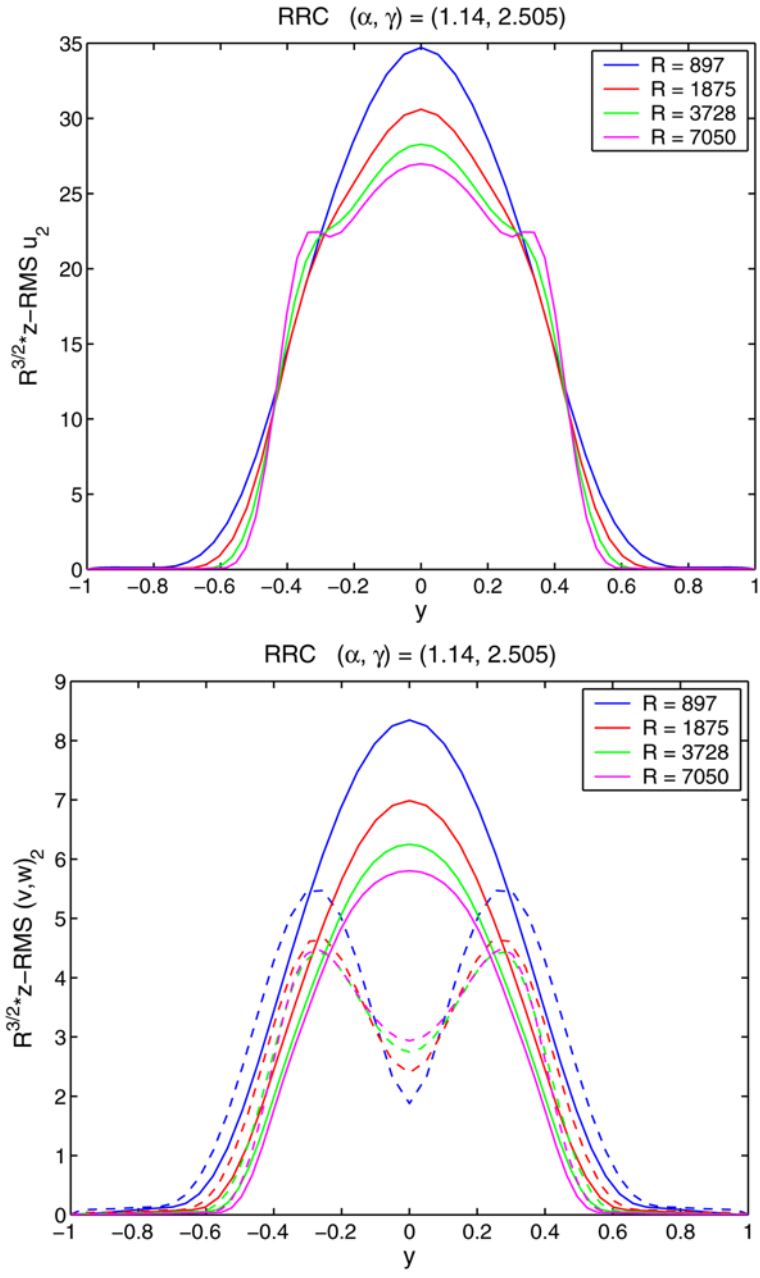

Figure 7. z-RMS velocity profiles scaled by $R^{3/2}$ for the 2nd harmonic $\boldsymbol{v}_2$. Top: $u_2(y, z)$. Bottom: v_2 solid, w_2 dash. Peak scaled rms decreases with increasing R for all three components.

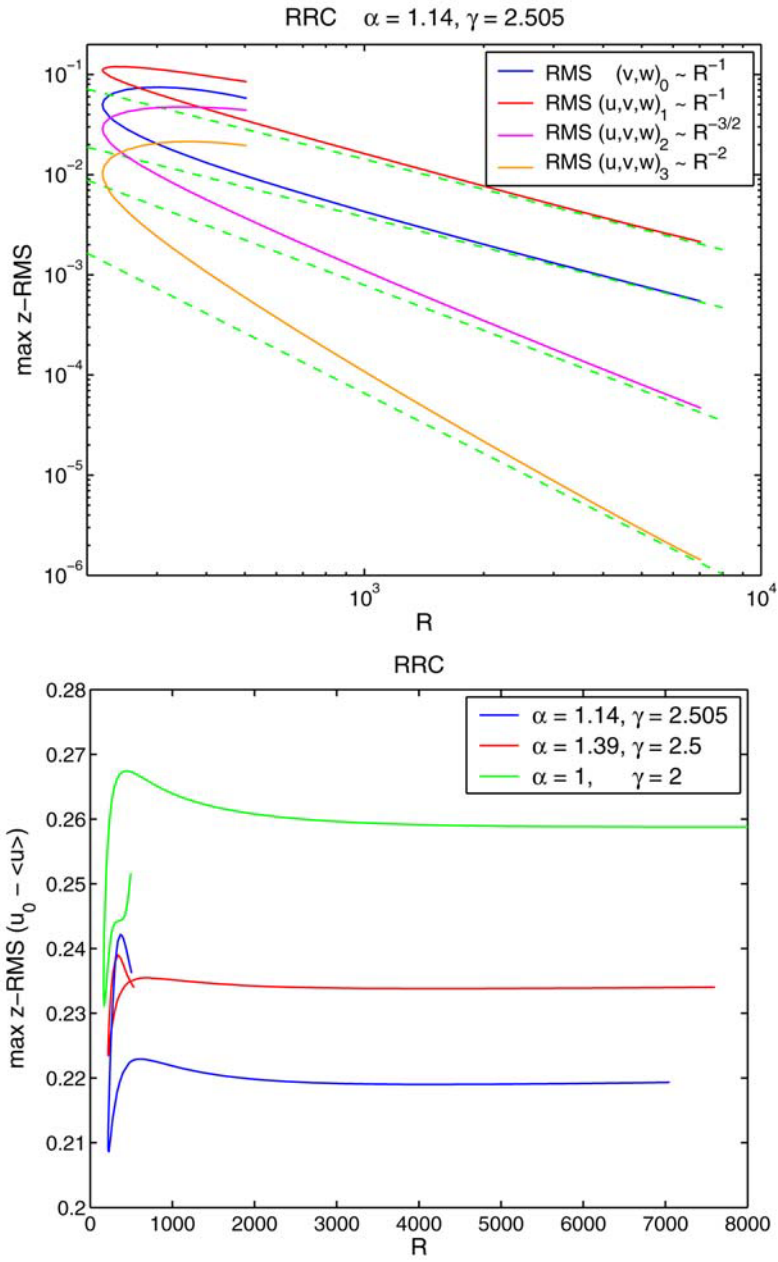

Figure 8. Peak z-rms velocity fluctuation profiles *vs.* R. Top: 1st harmonic, streamwise rolls, 2nd and 3rd harmonics (highest to lowest curve) for $(\alpha, \gamma) = (1.14, 2.505)$. Dashed lines: R^{-1} fits for $\boldsymbol{v}_1$ and rolls (v_0, w_0), $R^{-3/2}$ for $\boldsymbol{v}_2$ and R^{-2} for $\boldsymbol{v}_3$. Bottom: streaks $u_0(y, z) - \bar{u}(y)$ for $(\alpha, \gamma) = (1.14, 2.505)$ (lowest curve), (1.39,2.5) (middle), (1,2) (top curve). Composite of several resolutions, [9,75,21] for highest R.

to a finite value confirming that streaks remain $O(1)$ as $R \to \infty$. Other results for these other (α, γ) are similar to those reported here for (1.14, 2.505).

5. CONCLUSIONS

We have continued lower branch exact coherent structures in no-slip plane Couette flow to high Reynolds number, up to about 20 times higher than the Reynolds number ($\approx$ 320) where turbulence is first observed to occur. Our results support earlier presumptions that the lower branch coherent states have streaks of $O(1)$ supported by streamwise rolls and a streak eigenmode of $O(R^{-1})$. The numerical results show that the higher harmonics do not follow the naive scaling where the n-th harmonic would scale like R^{-n}. There is instead clear evidence for the importance of a critical layer determined by $u_0(y, z) - c = 0$ where $u_0(y, z)$ is the x-averaged streamwise velocity and c is the traveling velocity of the structure. This critical layer reduces the decay rate of the higher harmonics. The 2nd harmonic appears to decay like $R^{-3/2}$ and the 3rd harmonic like R^{-2}. Nonetheless, this suggests that the various harmonics separate as $R \to \infty$ and that the limiting state of the flow is given by a "mean flow-first harmonic theory" similar to that proposed by Benney (1984). In other words, the self-sustaining process (Figure 1) becomes exact for the lower branch states as $R \to \infty$. The flow retains an essential spanwise variation, sustained by ever weaker rolls and a single x-harmonic eigenmode of the streaky flow. The streaky flow never connects to the laminar flow, not even at infinity.

On the transition threshold question, we expect that all *lower branch* nontrivial states based on the self-sustaining process will have the same asymptotic scaling: $O(1)$ streaks supported by $O(R^{-1})$ rolls and streak eigenmode. This suggests that the best perturbations to trigger turbulence probably consist of channel size $O(R^{-1})$ streamwise rolls of streamwise extent of the order of a few channel sizes as well to trigger a first harmonic of the proper wavelength and strength (Figure 3). The relevant length scale ℓ is the full width in plane Couette, the half-width in plane Poiseuille and the radius in pipe flow, i.e. the width of the laminar shear layer. The jet perturbation used in Hof et al. (2003) precisely generates a disturbance of that form, i.e. a pair of counter-rotating vortices whose axes are aligned in the streamwise direction, provided the duration of the jet is at least of the order of the convective time scale ℓ/U. The SSP suggests that very short jets will not be very effective at triggering turbulence, since they would trigger α's that are too large and would not set up sufficiently long streaks. On the other hand, the SSP suggests there will be little sensitivity to the length of the pulse once it is longer than a few ℓ's, since sufficiently long rolls will have been excited leading to sufficiently long

naturally unstable streaks. This is entirely consistent with the results of Hof et al. (2003, fig. 3).

ACKNOWLEDGEMENTS

FW thanks Tom Mullin and Rich Kerswell for organizing the Bristol workshop and Julian Scott for discussions about critical layers at that workshop. This work was partially supported by the US NSF through grant DMS-0204636. FW thanks Beth Wingate, Susan Kurien and Bob Ecke for setting up an extended visit to Los Alamos National Laboratory where this article was written [LA-UR-04-8916].

NOTES

1. For transient growth, the essence of the WKB results can be obtained by considering the linear evolution of Kelvin modes, i.e. Fourier modes with time-dependent wavevectors, on an unbounded plane Couette flow.

2. Chapman assumes the predominance of nonlinear interactions between oblique streaks (rapidly oscillating in y) that would generate large scale streamwise rolls and between oblique streaks and streamwise streaks to sustain the oblique rolls (this is more clearly illustrated by his "toy model" (2.6)-(2.9) and his figures 19 and 20). This is an excitation of subharmonic-type where oblique modes with horizontal wavenumbers $(\pm\alpha, \gamma)$ would create a pair of streamwise rolls with spanwise wavenumber $(0, 2\gamma)$. In Chapman's oblique transition scenario, the oblique streaks are induced by velocity perturbations of $O(R^{-1})$ and $O(R^{-5/4})$, in Couette and Poiseuille flows, respectively, that rapidly oscillate in y on a $R^{-1/3}$ length-scale. Such perturbations correspond to rather intricate initial perturbations with vorticity of $O(R^{-2/3})$ and $O(R^{-11/12})$, much larger than the corresponding vorticity perturbations for the streamwise vortex scenario.

3. Chapman's "toy model" does incorporate feedback but his formal asymptotic study merely estimates the size of streamwise streaks necessary to perturb the laminar flow eigenvalues at lowest order, assuming but not demonstrating that this would lead to streak instability. His entire analysis ignores the modification of the mean shear. His nonlinear system (3.6), (3.12) is not complete since it lacks the equation for the mean flow. As recalled in the introduction, the mean shear perturbation is of order $(\epsilon R)^2$ which is of order unity for $a = -1$ and these mean flow modifications play an important role in the streak instability, at least in plane Couette flow (as discussed in Waleffe, 1995a, 1995b, 1997; Reddy et al., 1998).

4. Chapman's Couette analysis focuses on streamwise rolls of amplitude $\epsilon \sim R^{-1}$, as in the SSP (Figure 1), but that implies an order 1 reduction of the mean shear that invalidates linear theory about the laminar flow. Chapman's Poiseuille analysis suggests that large scale streamwise rolls of $O(R^{-3/2})$ are the most efficient to lead to streak instability. That threshold corresponds to odd-in-y streamwise rolls, that do *not* correspond to the largest transient growth. Although instability of the resulting $O(R^{-1/2})$ streaks is plausible, it has not been shown that instability of such streaks would lead to some feedback able to trigger transition.

5. The 4th order model is derived for a sinusoidal shear flow $(\sin \pi y/2, 0, 0)$ maintained by a body force. $M(t)$ represents the amplitude of that shear flow, $U(t)$ is the amplitude of a pure streak mode of the form $(\cos \gamma z, 0, 0)$ whose z-average vanishes, $V(t)$ is the amplitude of a streamwise roll of the form $(0, \gamma \cos \beta y \cos \gamma z, \beta \sin \beta y \sin \gamma z)$ while $W(t)$ is the amplitude of a streak eigenmode sinusoidal in x, but whose minimum representation involves 5 Stokes modes (see Waleffe, 1997, eqns. 8, 9 and sect. III, C). In the context of Section 3 and Equations (8), (9) and (10), $M(t)$ would represent a measure of the mean shear (i.e. y-derivative of the x and z averaged streamwise velocity, $\overline{u}^{xz}$, which is identical to $\overline{u_0}^z$, the z-average of $u_0(y, z)$) in a neighborhood of the critical layer $u_0(y, z) - c = 0$ (not near the no-slip walls), $U(t)$ would represent the amplitude of the streaks (i.e. of $u_0(y, z) - \overline{u_0}^z$), $V(t)$ would represent the amplitude of the unscaled rolls (i.e. $R^{-1}\psi_0(y, z)$) and $W(t)$ the amplitude of the unscaled streak eigenmode $(R^{-1}\boldsymbol{v}_1(x, y, z) + c.c.)$.

6. Since the Navier–Stokes numerical results indicate the presence of a critical layer, it is interesting to note that the scaling of the lower branch fixed point in the 4th order model would not change even if the decay rate of W was order $R^{-1/3}$, typical of linear critical layers and shear-induced diffusion, instead of R^{-1}.

7. The lower branch coherent state is a saddle fixed point with many stable but a few unstable directions. Its 'stable' manifold is the set of all initial conditions that will end up at the fixed point in forward time, but that manifold is unstable in the sense that initial conditions near but not on the 'stable' manifold will move away from that manifold.

REFERENCES

Acarlar, M.S. and Smith, C.R. (1987). A study of hairpin vortices in a laminar boundary layer. *J. Fluid Mech.* **175**, 1–41 and 45–83.

Benney, D.J. (1984). The evolution of disturbances in shear flows at high reynolds numbers. *Stud. Appl. Math.* **70**, 1–19.

Benney, D.J. and Chow, K.A. (1989). A mean flow first harmonic theory for hydrodynamic instabilities. *Stud. Appl. Math.* **80**, 37–73.

Chapman, S.J. (2002). Subcritical transition in channel flows. *J. Fluid Mech.* **451**, 35–97.

Eckhardt, B. and Mersmann, A. (1999). Transition to turbulence in a shear flow. *Phys. Rev. E* **60**, 509–517.

Faisst, H. and Eckhardt, B. (2003). Traveling waves in pipe flow. *Phys. Rev. Lett.* **91**, 224502.

Hamilton, J., Kim, J. and Waleffe, F. (1995). Regeneration mechanisms of near-wall turbulence structures. *J. Fluid Mech.* **287**, 317–348.

Hof, B., Juel, A. and Mullin, T. (2003). Scaling of the turbulence transition threshold in a pipe. *Phys. Rev. Lett.* **91**, 244502.

Itano, T. and Toh, S. (2001). The dynamics of bursting process in wall turbulence. *J. Phys. Soc. Japan* **70**, 703–716.

Joseph, D.D. and Tao, L.N. (1963). Transverse velocity components in fully developed unsteady flows. *J. Appl. Mech.* **30**, 147–148.

Kawahara, G. and Kida, S. (2001). Periodic motion embedded in plane Couette turbulence: Regeneration cycle and burst. *J. Fluid Mech.* **449**, 291–300.

Kreiss, G., Lundbladh, A. and Henningson, D.S. (1994). Bounds for threshold amplitudes in subcritical shear flows. *J. Fluid Mech.* **270**, 175–198.

Maslowe, S.A. (1986). Critical layers in shear flows. *Ann. Rev. Fluid Mech.* **18**, 405–432.

Moehlis, J., Faisst, H. and Eckhardt, B. (2004). A low-dimensional model for turbulent shear flows. *New Journal of Physics* **6**, 56+17.

Nagata, M. (1990). Three-dimensional finite-amplitude solutions in plane Couette flow: Bifurcation from infinity. *J. Fluid Mech.* **217**, 519–527.

Reddy, S.C., Schmid, P.J., Baggett, J.S. and Henningson, D.S. (1998). On stability of streamwise streaks and transition thresholds in plane channel flows. *J. Fluid Mech.* **365**, 269–303.

Trefethen, N., Trefethen, A.E., Reddy, S.C. and Driscoll, T.A. (1993). Hydrodynamic stability without eigenvalues. *Science* **261**, 578–584.

Waleffe, F. (1990). Proposal for a self-sustaining process in shear flows. Working paper, available at http://www.math.wisc.edu/∼waleffe/ECS/sspctr90.pdf.

Waleffe, F. (1995a). Hydrodynamic stability and turbulence: Beyond transients to a self-sustaining process. *Stud. Applied Math.* **95**, 319–343.

Waleffe, F. (1995b). Transition in shear flows: Nonlinear normality versus non-normal linearity. *Phys. Fluids* **7**, 3060–3066.

Waleffe, F. (1997). On a self-sustaining process in shear flows. *Phys. Fluids* **9**, 883–900.

Waleffe, F. (1998). Three-dimensional coherent states in plane shear flows. *Phys. Rev. Lett.* **81**, 4140–4148.

Waleffe, F. (2001). Exact coherent structures in channel flow. *J. Fluid Mech.* **435**, 93–102.

Waleffe, F. (2002). Exact coherent structures and their instabilities: Toward a dynamical-system theory of shear turbulence. In *Proceedings of the International Symposium on Dynamics and Statistics of Coherent Structures in Turbulence: Roles of Elementary Vortices*, S. Kida (ed.), National Center of Sciences, Tokyo, Japan, pp. 115–128.

Waleffe, F. (2003). Homotopy of exact coherent structures in plane shear flows. *Phys. Fluids* **15**, 1517–1543.

Waleffe, F., Kim, J. and Hamilton, J. (1993). On the origin of streaks in turbulent shear flows. In *Turbulent Shear Flows 8: Selected Papers from the Eighth International Symposium on Turbulent Shear Flows*, Munich, Germany, September 9–11, 1991, F. Durst, R. Friedrich, B.E. Launder, F.W. Schmidt, U. Schumann and J.H. Whitelaw (eds), Springer-Verlag, Berlin, pp. 37–49.

Wedin, H. and Kerswell, R.R. (2004). Exact coherent structures in pipe flow. *J. Fluid Mech.* **508**, 333–371.